Electronic Supplementary Material (ESI) for Journal of Materials Chemistry A.

Supporting Information

Highly selective Photocatalytic CO_2 Reduction via a Lead-free Perovskite/MOF Catalyst

Na Li, Xin-Ping Zhai, Bo Ma, Hui-Jie Zhang, Ming-Jun Xiao, Qiang Wang,* Hao-Li Zhang*

State Key Laboratory of Applied Organic Chemistry (SKLAOC), Key Laboratory of Advanced Catalysis of Gansu Province, College of Chemistry and Chemical Engineering, Key Laboratory of Special Function Materials and Structure Design, Ministry of Education, Lanzhou University, Lanzhou, 730000,China.

Correspondence authors:

qiangwang@lzu.edu.cn (Q.W.); haoli.zhang@lzu.edu.cn (H.-L.Z.)

1. Experimental Section

1.1 Materials: Chemicals

CsBr and $BiBr_3$ were purchased from Aladdin Chemistry Co. Ltd. tetrakis(4-carboxyphenyl)porphyrin and Zirconyl chloride octahydrate were purchased from Aladdin Chemistry Co. Ltd. Dimethyl sulfoxide (DMSO) was from Tianjin Rianlon Corporation Pharmaceutical& Chemical Co. Ltd. isopropanol was from Guangdong Fine Chemicals Engineering Technology Research Center Co. Ltd. All solvents and chemicals were used without any further purification. Deionized water with resistivity of 18.3 MΩ•cm was used to prepare aqueous solution throughout the experiment.

2. Photoelectrochemical Measurements

Photocurrent measurements were performed using a standard three-electrode cell with the as-prepared sample films as the working electrode, a platinum foil as the counter electrode, and a saturated Ag/AgCl as the reference electrode. 0.05 M tetrabutylammonium hexafluorophosphate ($TBAPF_6$)/ethyl acetate solution was filled in the quartz cell as the electrolyte. The photocurrents were recorded on a Zennium electrochemical workstation (Zahner) under irradiation of a 300 W Xe lamp (AM1.5G, and 100 $mW \cdot cm^{-2}$) at open circuit voltage.

3 Characterization methods

Spectroscopic measurement

The UV/Vis absorption spectra were obtained on a TU-1810 Spectrophotometer (Beijing Purkinje General Instrument, China). FTIR spectra were collected on a VERTEX 70V instrument. Both LS 55 fluorescence spectrometer (Perkin-Elmer) and for the femtosecond broadband pump-probe spectroscopy, the laser source was a Coherent Legend Elite regenerative amplifier (1 KHz, 800 nm) that was seeded by a Coherent Chameleon oscillator (110 fs, 80 MHz). $Cs_3Bi_2Br_9$ QDs and $Cs_3Bi_2Br_9$/MOF-525-Co were respectively drop-casted on quartz glasses as films for the transient

absorption tests. TCPP, MOF525 and MOF 525Co were dispersed in the DMF solvent for testing. All of the measurements were performed at room temperature unless otherwise specified.

Other characterizations

The TEM micrographs were obtained using Talos F200S Field Emission Transmission Electron Microscopes (FEI, USA) at operating voltages of 200 kV, respectively. Powder X-ray diffraction (XRD) patterns of the products were recorded on a Panalypical X' Pert PRO diffract meter using Cu Kα X-rays between 5° and 50°. X-ray photoelectron spectroscopy (XPS) and ultraviolet photoelectron spectroscopy (UPS) measurements were performed on an AXIS Ultra instrument.

The Co contents of composites were analyzed by inductively coupled plasma optical emission spectrometry (ICP-OES, 5110, Agilent Technologies Inc., USA).

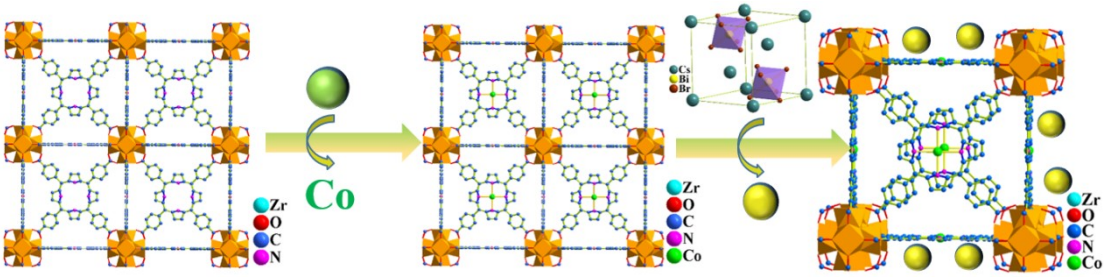

Scheme S1. Synthesis of Composite Catalysts $Cs_3Bi_2Br_9$/MOF 525 Co

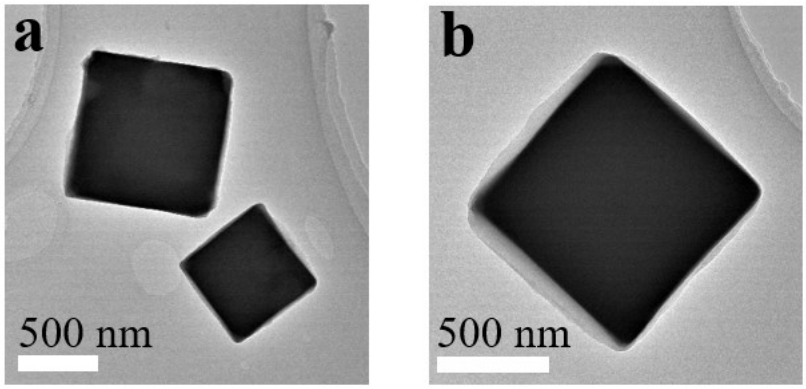

MOF 525 **MOF 525 Co**

Fig. S1. More representative TEM images of (a) MOF525, (b) MOF525Co.

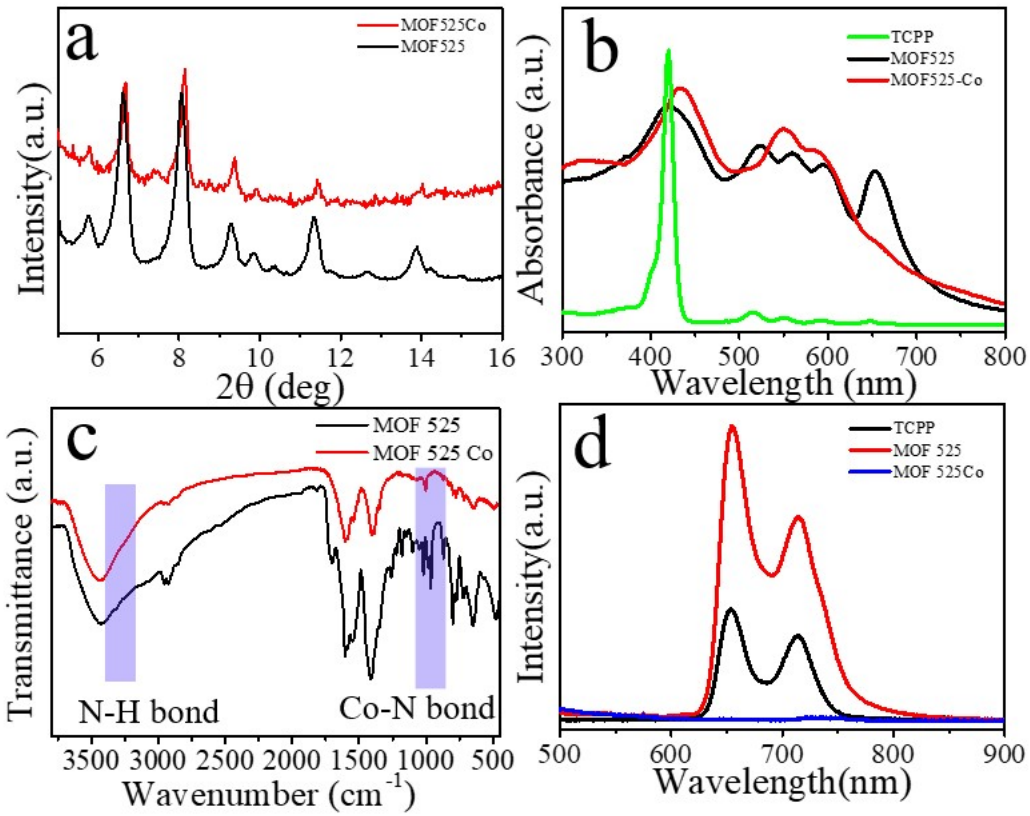

Fig. S2. The corresponding XRD patterns (a), UV-Vis spectra (b) and FT-IR spectra (c) of MOF525, MOF525Co, (d) Steady-state PL spectra of the TCPP, MOF525 and MOF525Co with an excitation wavelength of 375 nm.

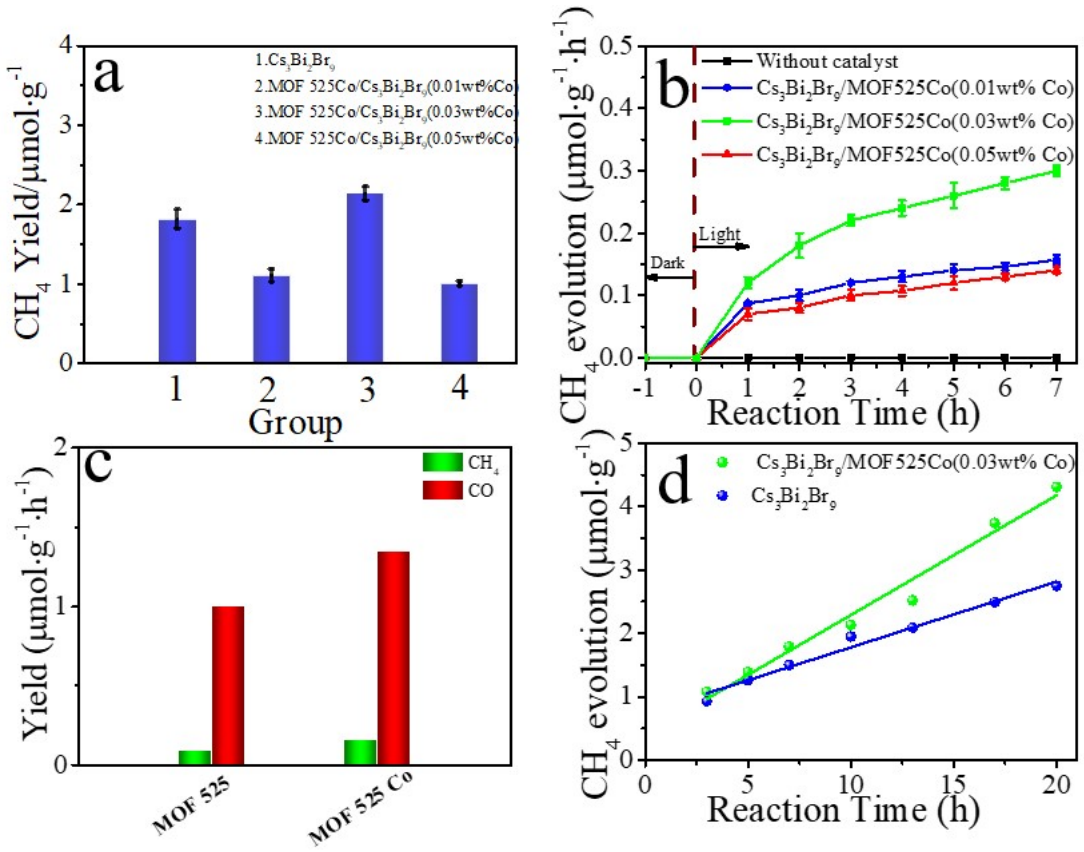

Fig. S3. Photocatalytic performance of for CO_2 reduction CH_4 yield (a) using different catalysts; (b) product yields within 7 h, (c) using MOF 525 and MOF525 Co catalysts, (d) Long-time catalytic stability of $Cs_3Bi_2Br_9$ QDs and the $Cs_3Bi_2Br_9$/MOF 525-Co (0.03 wt% Co).

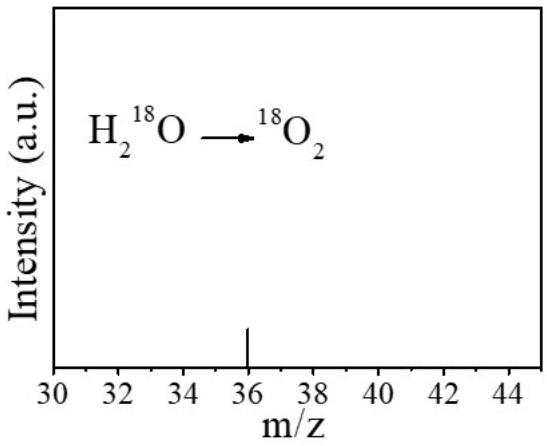

Fig. S4. Gas chromatography-mass spectrometric (GC-MS) analysis for solar-driven oxidation of $H_2{}^{18}O$ to $^{18}O_2$ (m/z = 36) using $Cs_3Bi_2Br_9$/MOF 525-Co (0.03 wt% Co) as a photocatalyst.

Apparent quantum efficiency (AQE) measurement

The AQE was measured according to the previous reported method.[1] We measured the AQE using the same experimental setup, but with 420 nm LED light source to obtain monochromatic light and the equation as follows:

$$AQE(\%) = \frac{Number\ of\ reacted\ electrons\ (N_{electron})}{Number\ of\ incident\ photons(N_{photon})} x100$$

The calculation of $N_{electron}$ is based on the fact that two electrons are required to produce one molecule CO, while 8 electrons for the one molecule CH_4, according to the equations mentioned in the manuscript. For $Cs_3Bi_2Br_9$/MOF 525 Co (0.03 wt% Co) catalyst, the CO and CH_4 production were 3.4 μmol and 0.2 μmol with 420 nm monochromatic light.

So, $N_{electron}$=2N (CO) +8N (CH_4) =2*3.4 μmol + 8*0.2 μmol =8.4 μmol

Number of incident photons are calculated using the following equations:

$$N_{photon} = \frac{Light\ intensity\ *\ Illumination\ area\ *\ Time}{Average\ single\ photonenergy\ *\ N_A}$$

$$= \frac{100\ mw \cdot cm^{-2} * 9.62\ cm^2 * 3600\ s}{\frac{6.625 \times 10^{-34} J \cdot s * 3 \times 10^{17} nm \cdot s^{-1}}{420\ nm} * 6.022 \times 10^{23} mol^{-1}} = 12155\ \mu mol$$

where the illumination area is controlled to 9.62 cm^2, N_A is the Avogadro constant and the average single photon energy (E_{photon}) is figured out using the equation: E_{photon}=hc/λ, where h is the Planck constant, c indicates speed of light, and λ is the wavelength.

Finally, $$AQE(\%) = \frac{8.4\ \mu mol}{12155\ \mu mol} x100 = 0.07\%$$

Under the same experimental conditions, for $Cs_3Bi_2Br_9$ QDs, the CO and CH_4 production were 2.4 μmol and 0.1 μmol.

Finally, $$AQE(\%) = \frac{5.6\ \mu mol}{12155\ \mu mol} x100 = 0.046\%$$

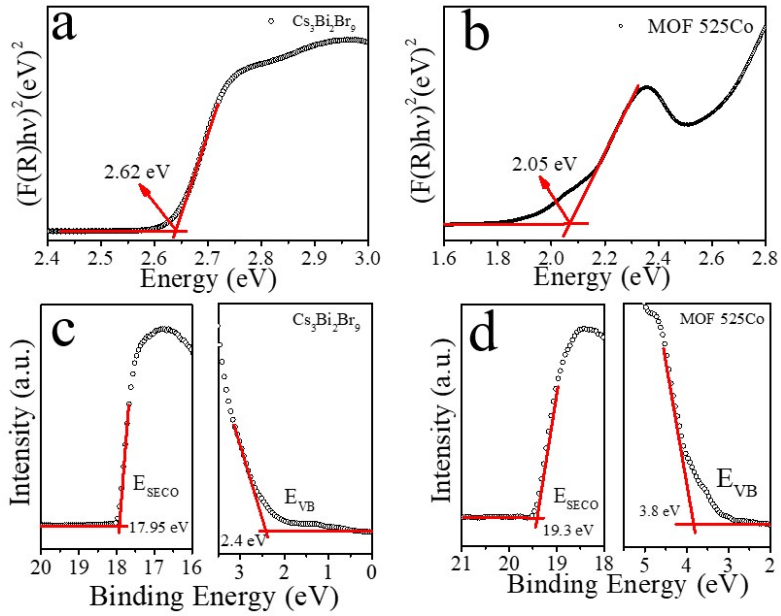

Fig. S5. The Tauc plot of $Cs_3Bi_2Br_9$ QDs (a) and MOF 525 Co (b) The Ultraviolet photoelectron spectra of $Cs_3Bi_2Br_9$ QDs (c) and MOF 525 Co (d).

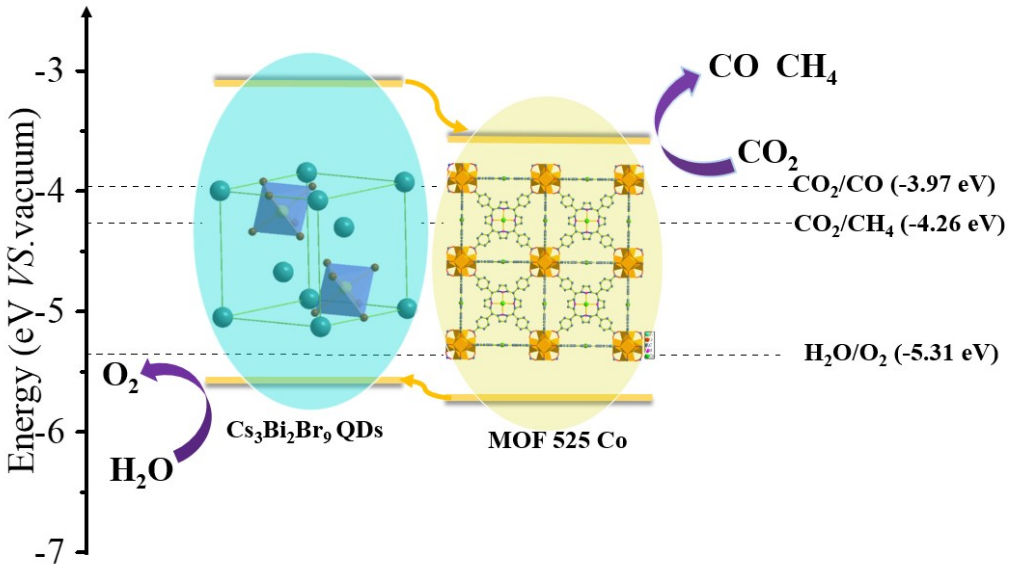

Fig. S6. The proposed photocatalytic procedure and electronic bandgap information for the type II heterojunction.

Table S1. A summary of the photocatalytic CO_2 reduction performance by metal halide perovskites photocatalysts.

Photocatalysts	Reaction condition	Light source	Products/ μmol g^{-1} h^{-1}	$R_{electron}$/ μmol g^{-1} h^{-1}	CO Selectivity (%)	Ref
$Cs_3Bi_2Br_9$/MOF-525-Co (0.03 wt% Co)	CO_2 and Water Vapor	AM 1.5G, 100 mW cm^{-2}	CH_4: 0.3 CO: 61.2	124.8	99.5	**This work**
Cs_2CuBr_4 QDs	CO_2 and Water Vapor	300W Xe AM1.5G	CH_4: 14.96 CO: 29.8	179.29	33.4	*ACS Catal*. 2022, 12, 2915-2926
$Cs_3Bi_2I_9$ QDs	Gas (CO_2+H_2O)	32 W UV Lamp 305 nm 80.38 μW/cm^2	CO: 7.8 CH_4: 1.5	27.6	83.8	*J. Am. Chem. Soc.*, 2019, 141, 20434-20442.
$M_{A3}Bi_2I_9$ QDs	Gas (CO_2+H_2O)	32 W UV Lamp 305 nm 80.38 μW/cm^2	CO: 0.7 CH_4: 1.0	9.4	41	*J. Am. Chem. Soc.*, 2019, 141, 20434-20442.
$Rb_3Bi_2I_9$ QDs	Gas (CO_2+H_2O)	32 W UV Lamp 305 nm 80.38 μW/cm^2	CO: 1.8 CH_4: 1.7	17.2	51	*J. Am. Chem. Soc.*, 2019, 141, 20434-20442.
$Cs_3Bi_2I_9$ QDs	Toluene	300 W Xe lamp AM1.5G	CO: 1.1	2.2	100	*ACS Nano* 2020, 14, 13103-13114
$Cs_3Bi_2Br_9$ QDs	Toluene	300 W Xe lamp AM1.5G	CO: 26.9	53.8	100	*ACS Nano* 2020, 14, 13103-13114
$Cs_3Bi_2Cl_9$ QDs	Toluene	300 W Xe lamp AM1.5G	CO: 16.6	33.2	100	*ACS Nano* 2020, 14, 13103-13114
$Cs_3Bi_2Br_9$@M-Ti	Isopropanol	300 W Xe lamp, 70 mW·cm^{-2}	CH_4: 28.8 CO: 4.84	240.08	85.6	*Angew. Chem. Int. Ed.*, 2022, 61, e202200872.
In_4SnS_8/ $Cs_3Bi_2Br_9$	Gas-solid reactor	300 W Xe lamp ＞420 nm	CO: 9.55	19.1	100	*Applied Catalysis B: Environmental* 313 (2022) 121426
$Cs_3Bi_2I_9/CeO_2$	Gas (CO_2+H_2O)	300 W Xe lamp 100 mW/cm^2	CH_4: 5.8 CO: 14	74	70.7	*J. Energy Chem.* , 2022, 69, 348-355.
Cs_2SnI_6/SnS_2	Gas (CO_2+H_2O+ CH_3OH)	100 W Xe lamp ＞400 nm 150 mW/cm^2	CH_4: 2.0	16.0	0	*J. Am. Chem. Soc.* 2019, 141, 13434-13441
$Cs_3Bi_2I_9/Bi_2WO_6$	Gas	300 W Xe lamp	CO: 7.3	14.6	100	

	(CO_2+H_2O)	100 mW/cm^2				*Sol. RRL*, 2021, 5, 2000691.
$Cs_2AgBiBr_6$ NC	EA	AM 1.5G, 150 mW cm^{-2}	CH_4: 2.35 CO: 1.6	22	40	*Small* 2018, 14, 1703762
Cs_2AgBiI_6	CO_2 and H_2O Vapor	300 W Xe lamp 420nm	CO: 6.3	12.6	100	*Chem. Mater.* 2021, 33, 13, 4971–4976
$Cs_2AgBiCl_6$	CO_2 and H_2O Vapor	-	CO: 4.54	9.08	100	-
$Cs_2AgBi(Br_{0.5}I_{0.5})_6$	CO_2 and H_2O Vapor	-	CO: 3.96	7.92	100	-
$Cs_2AgInCl_6$@Ag	EA	300 W Xe lamp	CH_4: 4.66 CO: 4.86	47	51	*Sustainable Energy & Fuels* 2021**,** 5 (14), 3598-3605
$Cs_2AgBiBr_6$/Ce-UiO-66	CO_2 and H_2O Vapor	300W Xe AM1.5G	CO: 309.01 CH_4: 0.71	444.62	99	*Chem. Eng. J.*, 2022, 446, 137102.
$Cs_2AgBiBr_6$/Sr_2FeNbO_6	EA + Water	300W Xe Lamp $\lambda \geq 420$nm	CH_4: 8.12 CO: 50	164.96	86	*Chem. Eng. J.*, 2022, 446, 137197
$Cs_2AgBiBr_6$//Bi_2WO_6	EA+ Isopropanol	300W Xe Lamp	CH_4: 0.41 CO: 42.19	87.66	99	*Journal of Colloid and Interface Science*, 2023, 629, 233-242.
$Cs_2NaBiCl_6$	CO_2 and H_2O Vapor	300W Xe Lamp	CH_4: 1.2 CO: 30	69.4	96	*Adv. Energy Mater.* 2022, 2202074

The catalytic performances of samples were calculated according to the total weight of materials.

The electron consumption yield was calculated with the following equation:

$Yield\text{electron} = 2Yield\text{CO} + 8Yield\text{CH}_4$

The CO selectivity was calculated from the product yield as follows:

CO selectivity = $R(CO)/[R(CO) + R(CH_4)] \times 100\%$, where R_{CO} and R_{CH4} represent the production rates of CO and CH_4, respectively.

Table S2. Fitted TA lifetimes of the $Cs_3Bi_2Br_9$ QDs and $Cs_3Bi_2Br_9$/MOF 525-Co

Sample	Wavelength(nm)	τ_1 (A_1)	τ_2 (A_2)	τ_3 (A_3)
$Cs_3Bi_2Br_9$ QDs	455 nm	2.9 ps (55.7%)	45.9 ps (29%)	13 ns (15.3%)
$Cs_3Bi_2Br_9$/MOF 525-Co	450 nm	2.6 ps (70.3%)	34.3 ps (21.4%)	7.5 ns (8.3%)
$Cs_3Bi_2Br_9$ QDs	468 nm	8.0 ps (49.3%)	40.6 ps (22.4%)	15.9 ns (28.3%)
$Cs_3Bi_2Br_9$/MOF 525-Co	471 nm	9.1 ps (84.3%)	22.3 ps (3.9%)	12.6 ns (11.8%)

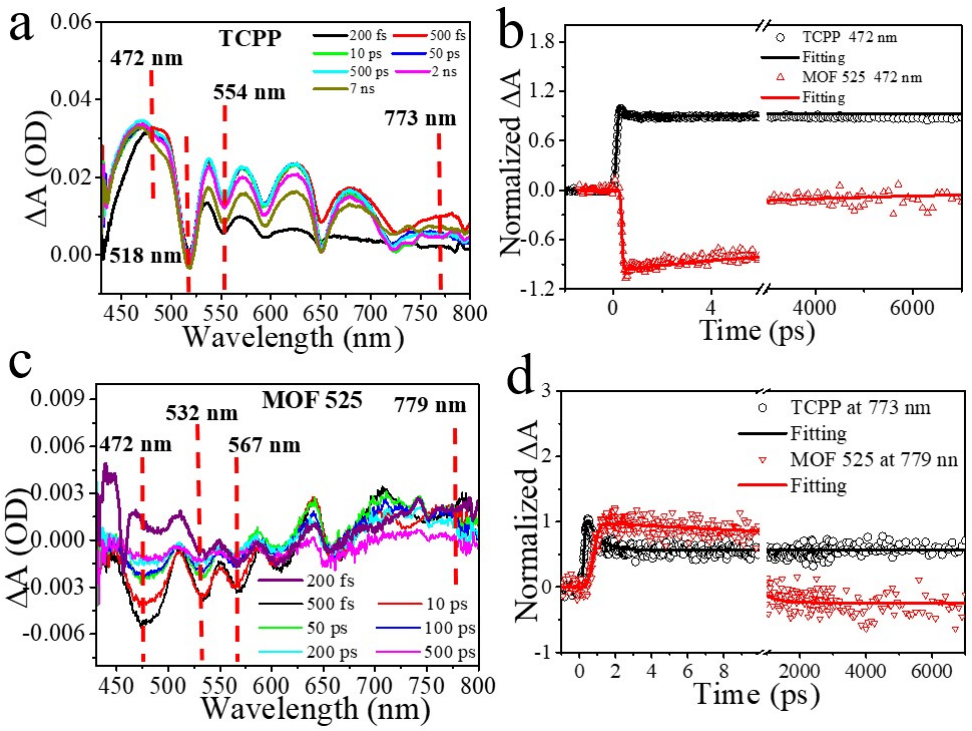

Fig. S7. Representative spectra at different delay time for TCPP(a) and MOF 525 (c) in the range of 200 fs-5 ns excited at 400 nm. Decay curves are normalized to the maximum signals at wavelengths of ~472 nm (b) and ~770 nm (d).

Table S3. Fitted lifetime componnets of TCPP and MOF 525.

Sample	Wavelength(nm)	$\tau_1(A_1)$	$\tau_2(A_2)$	$\tau_3(A_3)$
MOF 525	472 nm (S band)	7.1 ps (26.1%)	133 ps (50.2%)	>ns (23.7%)
TCPP	472 nm (S band)	124 fs (37.6%)		>ns (62.4%)
MOF 525	532 nm (Q1 band)	15.6 ps (31.2%)	156 ps (40.4%)	>ns (28.4%)
TCPP	518 nm (Q1 band)	10.7 ps (7.9%)	4.0 ns (-39.6%)	>ns (52.5%)
MOF 525	567 nm (Q2 band)	8.9 ps (24.7%)	111 ps (42.3%)	>ns (33%)
TCPP	554 nm (Q2 band)			>ns (100%)
MOF 525	779 nm	21.1 ps (22.2%)	466 ps (61.3%)	>ns (16.5%)

TCPP	773 nm	742 fs (52.1%)	>ns (47.9%)

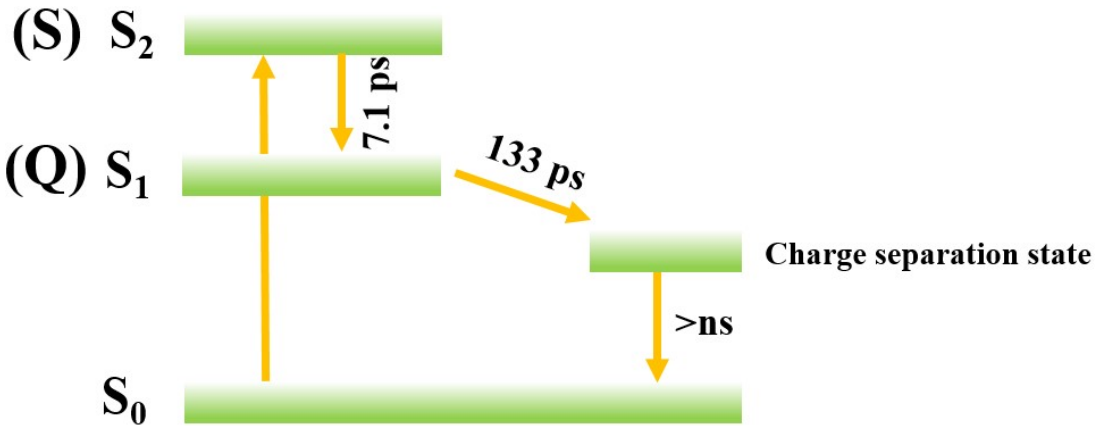

Fig. S8. Proposed dynamic steps within MOF525 upon photoexcitation. Herein the fitted lifetime at 472 nm (S band) at the 472 nm is taken as an example.

$$CO_2 \longrightarrow CO_2^*$$

$$H_2O \longrightarrow H^+ + OH^-$$

$$CO_2^* + e^- + H^+ \longrightarrow COOH^*$$

$$COOH^* + e^- + H^+ \longrightarrow CO^* \text{ or } CH_3{}^*O + H_2O$$

$$CO^* + e^- + H^+ \longrightarrow CO$$

$$CH_3{}^*O + e^- + H^+ \longrightarrow CH_4 + O^*$$

Scheme S2. The conversion process of photocatalytic CO_2 reduction[2]

References

[1] Fang, Z.-B.; Liu, T.-T.; Liu, J.; Jin, S.; Wu, X.-P.; Gong, X.-Q.; Wang, K.; Yin, Q.; Liu, T.-F.; Cao, R.; Zhou, H.-C., Boosting Interfacial Charge-Transfer Kinetics for Efficient Overall CO_2 Photoreduction via Rational Design of Coordination Spheres on Metal–Organic Frameworks. *J. Am. Chem. Soc.* **2020**, *142* (28), 12515-12523.

[2] Ding, L.; Bai, F.; Borjigin, B.; Li, Y.; Li, H.; Wang, X., Embedding $Cs_2AgBiBr_6$ QDs into Ce-UiO-66-H to in situ construct a novel bifunctional material for capturing and photocatalytic reduction of CO_2. *Chem. Eng. J.* **2022**, *446*, 137102.